Journal of Power Sources 238 (2013) 53–56

Contents lists available at SciVerse ScienceDirect

Journal of Power Sources

journal homepage: www.elsevier.com/locate/jpowsour

Short communication

All-solid-state lithium ion battery using garnet-type oxide and Li_3BO_3 solid electrolytes fabricated by screen-printing

Shingo Ohta*, Shogo Komagata, Juntaro Seki, Tohru Saeki, Shinya Morishita, Takahiko Asaoka

Toyota Central R&D Labs. Inc., Battery & Cells Div., 41-1 Yokomichi, Nagakute, Aichi 480-1192, Japan

HIGHLIGHTS

- All-solid-state battery with garnet-type oxide was constructed by screen printing process.
- LBO acts as the solid electrolyte and also as a bonding material in electrode layer.
- Sufficient interface contact between cathode and solid electrolyte can be easily achieved.
- This battery has good charge–discharge performance.
- Lower interfacial resistance between cathode and solid electrolyte was shown.

ARTICLE INFO

Article history:
Received 10 December 2012
Received in revised form
21 February 2013
Accepted 25 February 2013
Available online 21 March 2013

Keywords:
Lithium ion secondary battery
All-solid-state lithium ion battery
Solid oxide electrolyte
Electrochemical performance
Solid state reaction

ABSTRACT

An all-solid-state lithium ion battery was constructed with a screen-printing process using Nb doped $Li_7La_3Zr_2O_{12}$ (LLZONb) as the solid electrolyte and Li_3BO_3 (LBO) as a solid electrolyte within the cathode layer. LBO is a lithium ion conductor that is chemically stable with the $LiCoO_2$ (LCO) active cathode material and LLZONb. Sufficient interface contact between the cathode layer and the LLZONb solid electrolyte can be easily achieved with sintering LBO into the cathode layer by an annealing process. The resultant battery exhibited good electrochemical performance and a lower interfacial resistance comparable with that of lithium ion batteries with liquid organic electrolytes.

1. Introduction

All-solid-state lithium ion batteries containing solid electrolytes are considered to be safe due to their nonflammability. In addition, solid oxide electrolytes are believed to have a potential advantage over other inorganic materials in terms of their chemical stability, for example, they do not release toxic gases when decomposed. All-solid-state lithium ion batteries with solid oxide electrolytes have attracted significant attention due to these advantages.

The $Li_7La_3Zr_2O_{12}$ (LLZO) lithium garnet-like oxide was first reported by Murugan et al. in 2007 [1], and their derivatives [2–8] have attracted increasing attention as solid oxide electrolytes for all-solid-state lithium ion batteries due to their chemical stability, high lithium ion conductivity and wide potential window. LLZO with an optimized composition by niobium doping exhibits the highest lithium ion conductivity of approximately 0.8 mS cm^{-1} at 25 °C among the reported garnet-like oxides [9].

To assess the feasibility of Nb doped LLZO (LLZONb) as a solid oxide electrolyte for an all-solid-state lithium ion battery, we investigated the electrochemical performance and charge transfer resistance of a battery with LLZONb constructed by pulsed laser deposition method, because the dominant contributor to the internal resistance is the interfacial resistance between the electrodes and the solid electrolyte [10–13]. The all-solid-state lithium ion battery with LLZONb exhibited good charge–discharge capacities and lower interfacial resistance between electrodes and LLZONb comparable with that of lithium ion batteries with liquid organic electrolytes [14]. Thus, LLZONb is a promising candidate as a solid oxide electrolyte for all-solid-state lithium ion batteries.

It is generally considered that practical all-solid-state lithium ion batteries should be fabricated by a solid-phase fabricating process. However, the electrochemical performance and interfacial

* Corresponding author. Tel.: +81 561 71 7659; fax: +81 561 71 5743.
E-mail address: sohta@mosk.tytlabs.co.jp (S. Ohta).

0378-7753/$ – see front matter © 2013 Elsevier B.V. All rights reserved.
http://dx.doi.org/10.1016/j.jpowsour.2013.02.073

resistance of an all-solid-state lithium ion battery is strongly affected by the interfacial contact between the electrodes and electrolyte [15,16]. Therefore, the electrochemical performance of an all-solid-state lithium ion battery with an oxide electrolyte that was constructed by solid state reactions would still be lower than that of lithium ion battery with conventional liquid organic electrolytes. Thus, it is important to form an interface with high adhesion and contact between polycrystalline powders using, for example, sintering aids by a solid-phase fabricating process.

We have considered that Li_3BO_3 (LBO) would be a promising material to produce good interfacial contact in an all-solid-state lithium ion battery by a solid-phase fabricating process for the following reasons. This is primarily because LBO has a low melting point (ca. 700 °C) and is expected to act as a bonding material at the interface by melting. In addition, LBO is a lithium ion conductor. Therefore, LBO could be used as an electrolyte in the cathode layer. In this investigation, we have attempted to construct an all-solid-state lithium ion battery by a screen printing process, which is a one of a solid-phase fabricating process, using LBO as the solid electrolyte and also as a bonding material in positive electrode layer.

2. Experimental

LLZONb as a solid electrolyte (ca. 1 mm thick, 12 mm diameter bulk pellet) was fabricated by conventional solid-state reaction [8]. LBO was synthesized by ball-milling a mixture of Li_2CO_3 and B_2O_3, and then sintering at 600 °C for 10 h. The crystal structure and lattice parameters of the samples were evaluated by X-ray diffraction (XRD) analysis using Cu Kα radiation. LCO powder (average particle size: 5 μm, Nippon Chemical Industrial Co., Ltd.) was used as the active cathode material. To investigate the chemical stability of LBO with LCO and LLZONb, LBO was mixed with LCO or LLZONb powder in a 1:1 ratio (mol%) and heated at 700 °C. All-solid-state lithium ion batteries were constructed by the screen printing process. A screen printing paste of the cathode layer material was prepared by mixing LCO and LBO powder in a 75:25 (wt.%), with ethyl cellulose as a binder. The paste was then printed on the top side of the LLZONb pellet and annealed at 700 °C for 1 h to melt the LBO and remove any organic materials. Lithium metal as the active anode material was deposited on the opposite side of the LLZONb pellet using a vacuum deposition process. The morphology of the electrode/electrolyte interface of the battery was observed using field emission-scanning electron microscopy (FE-SEM; Hitachi S-5500). The electrochemical properties, such as the charge and discharge characteristics, were evaluated under galvanostatic conditions of 10 μA cm^{-2} (rate: 0.05 C) in the 4.05–3.0 V range at 25 °C using a potentio–galvanostat (Solartron 1480). The interfacial resistance of the battery was measured using an impedance analyzer (Solartron FRA 1255B) in the frequency range from 1 MHz to 0.1 Hz.

3. Results and discussion

Fig. 1 shows an XRD pattern of the synthesized LBO sample together with the standard pattern for LBO reported by the Joint Committee on Powder Diffraction Standards (JCPDS: PDF#01-070-2459). Although there were a few peaks that could not be assigned, the major phase was indexed as LBO. The chemical stability of LBO with LCO and LLZONb was investigated be heating mixtures at 700 °C. Neither of the mixtures was discolored after heating and no impurity peaks were evident from XRD measurements. Thus, LBO was determined to be chemically stable with both LCO and LLZONb.

The resistance of LBO was measured in vacuum using a two-probe AC impedance method. The LBO specimen was prepared by grinding LBO powder and pressing into a pellet. The LBO pellet was placed on an Au plate as an electrode and was melted by heating at

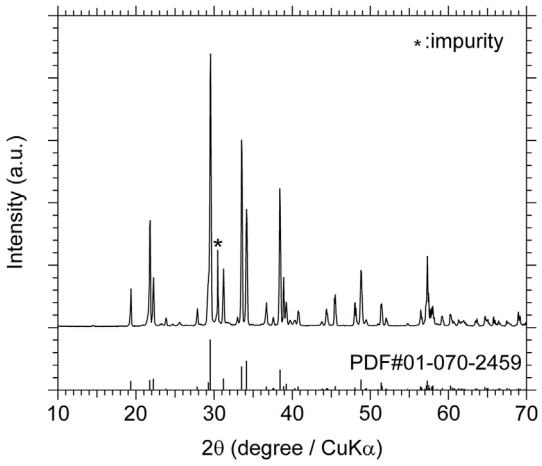

Fig. 1. XRD pattern of the Li_3BO_3 sample.

700 °C in air. After cooling to room temperature, an Au electrode was deposited on the top side of the LBO specimen using an ion sputter coater. Fig. 2a shows a Nyquist plot of LBO measured at 25 °C. The resistance of LBO was obtained from the intersection of the low frequency semicircle with the real axis at approximately 10 Hz. The appearance of a tail below 10 Hz suggests that the Au electrode blocked mobile ions. The temperature dependence of the ion conductivity for LBO is shown in Fig. 2b. The ion conductivity was linear and obeyed the Arrhenius law ($\sigma = A\exp(-E_a/kT)$, where A is the frequency factor, k is the Boltzmann constant, T is the absolute temperature, and E_a is the activation energy), which indicates that no structural or phase changes occurred in the observed temperature range. The resistivity at 25 °C and the activation energy were ca. 2×10^{-6} S cm^{-1} and 60 kJ mol^{-1}, respectively, which is comparable to that previously reported [17].

Fig. 3 presents cross-sectional FE-SEM (secondary electron and back scattered secondary electron (BSE)) images of the interface between the cathode and LLZONb solid electrolyte. The cathode layer consists of LCO and LBO fabricated by screen printing and annealed at 700 °C. The thickness of the cathode layer is approximately 10 μm. The distribution of LCO and LBO was clearly visible from the contrast of the BSE image. LBO was observed among LCO particles and between LCO and the LLZONb solid electrolyte, because LBO was melted during annealing process and would flow

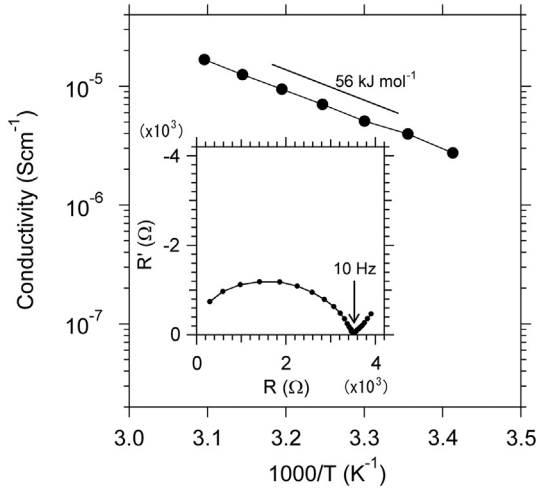

Fig. 2. Temperature dependence of the lithium ion conductivity for Li_3BO_3. Inset shows a Nyquist plot for Li_3BO_3 at 25 °C.

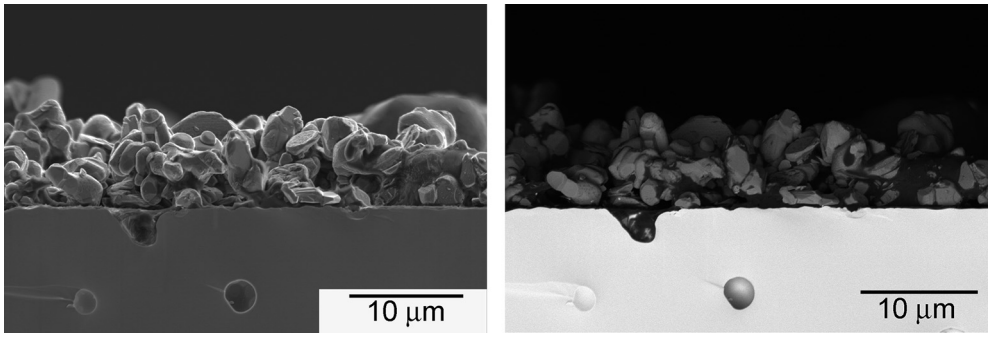

Fig. 3. Cross-sectional SEM images of secondary electron (left) and backscattering electron (right) images of the interface between the positive electrode layer ($LiCoO_2$ cathode active material and Li_3BO_3 solid electrolyte) and the $Li_{6.75}La_3Zr_{1.75}Nb_{0.25}O_{12}$ solid electrolyte.

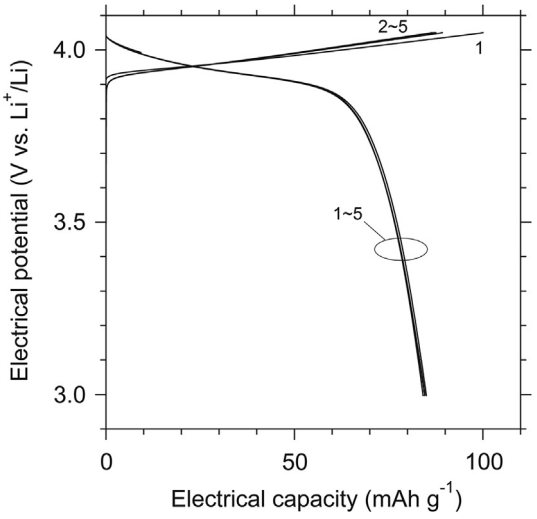

Fig. 4. Charge–discharge curves for the all-solid-state lithium ion battery. The horizontal axis shows the capacity normalized according to the weight of the $LiCoO_2$ cathode. The numbers in the figure indicate the cycle number.

into voids or into the interface spaces between LCO and LLZONb. No exfoliation or pores were observed at the interface, which indicates that this battery has sufficient interfacial contact between the electrolyte and the cathode layer.

Fig. 4 shows charge–discharge curves for the all solid state lithium ion battery up to the 5th cycle under galvanostatic conditions at 25 °C. The current density was 10 μA cm^{-2} (rate: ca. 0.05 C) and the discharging cutoff potentials was set at 3.0 V (vs. Li/Li^+). The charging cutoff potential was selected at 4.05 V (vs. Li/Li^+) to avoid unwanted phase transition of $LiCoO_2$ because it was well known that the crystal structure of $LiCoO_2$ changes from rhombohedral to monoclinic phase when Li content becomes under 0.45 per formula unit [18]. The charge and discharge capacities at the 1st cycle were 100 and 85 mAh g^{-1}, respectively. The theoretical electrochemical capacity of LCO is 115 mAh g^{-1}, which corresponds to 0.42 Li per CoO_2. Thus, the discharge capacity is approximately 74% of the theoretical capacity. The coulombic efficiency of the 1st charge–discharge cycle was approximately 85%, because the current due to the oxidative degradation of organolithium compounds generated during the annealing process was added to the first charging capacity. The coulombic efficiency after the 2nd cycle reached almost 100%. The discharge capacities from the 1st to 5th cycles were almost the same, which confirms the stable cycle performance of this battery.

The internal resistance of the battery was measured using the two-probe AC impedance method. Measurement was conducted after charging at 4.05 V vs. Li/Li^+. A Nyquist plot for the battery is shown in Fig. 5a. One resistance component and one semicircle appear with frequencies at approximately 0.5 MHz and 1 Hz, respectively. The resistance component at approximately 0.5 MHz, which was 80 Ω cm^2 at 25 °C, can be well-resolved into the resistance of the LLZONb bulk (R_{LLZONb}) [14]. The resistance that appeared as one semicircle was assumed to be a complex resistance due to the following resistance components: 1) the LBO bulk (R_{LBO}), 2) the interface between LCO and LLZONb ($R_{LCO/LLZONb}$), 3) the interface between LBO and LLZONb ($R_{LBO/LLZONb}$), 4) the interface between LCO and LBO ($R_{LCO/LBO}$) and 5) the interface between Li and LLZONb ($R_{Li/LLZONb}$). The frequency of the LBO

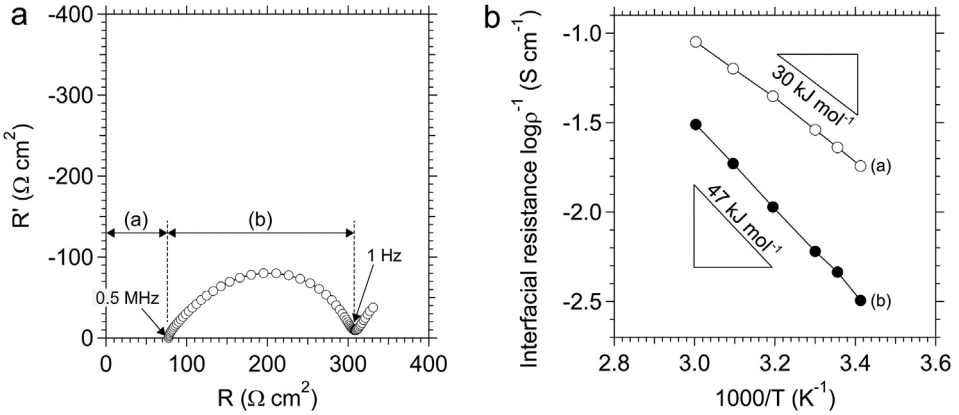

Fig. 5. a: Nyquist plot (0.1 Hz–1 MHz) for the all-solid-state lithium ion battery measured at 4.05 V, where (a) is the resistance of the LLZONb bulk electrolyte, and (b) incorporates both the interfacial resistance and the LBO bulk resistance. b: Temperature dependence of the resistivity (ρ) for resistance components (a) and (b).

bulk resistance was approximately 10 Hz (Fig. 2). The frequency dependence of $R_{Li/LLZONb}$ and $R_{LCO/LLZONb}$ are known to be 100 and 1 Hz, respectively [14]. Although the frequency dependence of $R_{LBO/LLZONb}$ and $R_{LCO/LBO}$ are still unknown, each resistance lies in almost the same range due to the heterointerface between oxides. The resistivity that appeared as a semicircle was 230 Ω cm^2 at 25 °C, which is comparable to the resistances of other interfaces between cathodes and other oxide electrolytes such as LCO and LiPON fabricated by physical vapor deposition method [19]. The temperature dependence of R_{LLZONb} (a) and the complex resistance (semicircle (b)) are shown in Fig. 5b. The E_a for the resistance of the latter was ca. 47 kJ mol^{-1}, which was larger than that for $R_{LCO/LLZONb}$ or $R_{Li/LLZONb}$ [14], and which was also smaller than that for R_{LBO} (ca. 56 kJ mol^{-1} (Fig. 2b)). Thus, it should be recognized that the resistance which appeared as a semicircle was not dominated by one component, but influenced by multiple components.

4. Conclusions

An all-solid-state lithium ion battery was constructed by screen-printing process using LLZONb as solid electrolyte and LBO as a solid electrolyte in the cathode layer. Sufficient interfacial contact between the cathode layer and LLZONb was easily formed by LBO melted during the annealing process. The charge and discharge capacities of the battery were approximately 74% of the theoretical capacity. The battery has a high coulombic efficiency and the resistance of the battery is comparable to that for a lithium ion battery constructed by the physical vapor deposition process. This result demonstrates that an all-solid-state lithium ion battery constructed by solid phase reaction process can have an electrochemical performance comparable with that of a lithium ion battery constructed by the physical vapor deposition process.

References

[1] R. Murugan, V. Thangadurai, W. Weppner, Angew. Chem. Int. Ed. 46 (2007) 7778.
[2] V. Thangadurai, H. Kaack, W. Weppner, J. Am. Ceram. Soc. 86 (2003) 437.
[3] V. Thangadurai, W. Weppner, Adv. Funct. Mater. 15 (2005) 107.
[4] V. Thangadurai, W. Weppner, J. Am. Ceram. Sic 88 (2005) 411.
[5] V. Thangadurai, W. Weppner, J. Power Sources 142 (2005) 339.
[6] R. Murugan, V. Thangadurai, W. Weppner, Ionics 13 (2007) 195.
[7] H. Xie, K.S. Park, J. Song, J.B. Goodenough, Electrochem. Commun. 19 (2012) 135.
[8] A. Logéata, T. Köhlera, U. Eiselea, B. Stiasznya, A. Harzera, M. Tovarb, A. Senyshync, H. Ehrenbergd, B. Kozinskye, Solid State Ionics 206 (2012) 33.
[9] S. Ohta, T. Kobayashi, T. Asaoka, J. Power Sources 196 (2011) 3342.
[10] K. Takada, T. Inada, A. Kajiyama, H. Sasaki, S. Kondo, M. Watanabe, M. Murayama, R. Kanno, Solid State Ionics 158 (2003) 269.
[11] N. Ohta, K. Takada, L.-Q. Zhang, R.-Z. Ma, M. Osada, T. Sasaki, Adv. Mater. 18 (2006) 2226.
[12] N. Ohta, K. Takada, I. Sakaguchi, L. Zhang, R. Ma, K. Fukuda, M. Osada, T. Sasaki, Electrochem. Commun. 9 (2007) 1486.
[13] A. Sakuda, H. Kitaura, A. Hayashi, K. Tadanaga, M. Tatsumisago, Electrochem. Solid-State Letters 11 (2008) A1.
[14] S. Ohta, T. Kobayashi, J. Seki, T. Asaoka, J. Power Sources 202 (2012) 332.
[15] M. Kotobuki, H. Munakata, K. Kanamura, Y. Sato, T. Yoshida, J. Electrochem. Soc. 157 (2010) A1076.
[16] M. Kotobukia, K. Kanamuraa, Y. Satob, K. Yamamotoa, Toshihiro Yoshidab, J. Power Sources 199 (2012) 346.
[17] M. Tatsumisago, N. Machida, T. Minami, Yogyo-Kyokai-shi 95 (1987) 197.
[18] T. Ohzuku, A. Ueda, J. Electrochem. Soc. 141 (1994) 2972.
[19] Y. Iriyama, T. Kako, C. Yada, T. Abe, Z. Ogumi, Solid State Ionics 176 (2005) 2371.